Neutrino-induced reaction rates for *r*-process nuclei

A. Hektor,[1] E. Kolbe,[2] K. Langanke,[1] and J. Toivanen[1]
[1]*Institute for Physics and Astronomy, University of Aarhus, Denmark*
[2]*Departement für Physik und Astronomie, Universität Basel, Switzerland*
(Received 6 December 1999; published 21 April 2000)

Neutrino-induced charged- and neutral-current reactions play an important role during and after the *r* process, if the latter occurs in an environment with extreme neutrino fluxes such as the neutrino-driven wind model or neutron star mergers. Therefore consistent *r*-process simulations require the knowledge of neutrino-nucleus reaction rates for very neutron-rich nuclei. The neutrino reactions can excite the daughter nucleus above the neutron threshold, which are quite low for *r*-process nuclei. Thus the daughter nucleus will decay by emission of one or several neutrons. We have calculated the relevant total and partial neutron spallation cross sections for *r*-process nuclei with neutron numbers $N=41-135$. Our calculations are based on the random phase approximation and consider allowed as well as forbidden transitions.

PACS number(s): 26.30.+k, 21.60.Jz, 23.40.Bw, 25.30.Pt

I. INTRODUCTION AND MOTIVATION

About half of the elements heavier than mass number $A=60$ are made in the astrophysical *r* process [1,2]. Empirically, the *r* process is rather well understood as a sequence of neutron-capture reactions and competing β decays, starting from a seed nucleus (e.g., ^{56}Fe). Simulations revealed that the *r* process proceeds through nuclei with approximately constant neutron separation energies ($S_n=2-3$ MeV) [3,4], far off the valley of stability. Thus, the realization of the *r* process in nature requires environments with extremely high neutron densities, usually associated with explosive events.

Despite impressive progress in the general understanding, the actual site of the *r* process has not yet been definitively identified. The currently favored scenario relates the *r* process to the high-entropy radiation bubble above the newly born neutron star in a type-II supernova [5,6] (neutrino-driven wind model). Although this site appears to be quite promising, several open questions and inconsistencies still remain to be solved. Therefore, neutron star mergers are actively investigated as alternative sites [7]. Both sites have in common that the *r* process will occur in the presence of extreme neutrino fluxes. We will exemplify for the neutrino-driven wind model the important aspects which neutrino-induced reactions on nuclei can play.

In a type-II supernova the neutron star remnant radiates its energy away via neutrino-antineutrino pairs which are produced with equal luminosity for all three neutrino flavors. However, charged-current reactions with the surrounding neutron-rich matter introduce differences in the neutrino opacities for the various neutrino species resulting in distinct differences in the neutrino distributions after these have diffused out of the neutron star. As ν_μ and ν_τ neutrinos and their antiparticles (combined referred to as ν_x neutrinos) decouple at the smallest radius in the star, their distribution has the largest average energy ($\overline{E}=25$ MeV). Electron neutrinos and antineutrinos interact with neutrons and protons in the dense matter via $n+\nu_e \rightarrow p+e^-$ and $p+\overline{\nu}_e \rightarrow n+e^+$, respectively. As the matter is neutron-rich, $\overline{\nu}_e$ neutrinos can decouple deeper in the star and they leave with a larger average energy ($\overline{E}=16$ MeV) than ν_e neutrinos ($\overline{E}=11$ MeV). These latter two reactions ensure also that the matter entering the radiation bubble has a neutron excess [8], i.e., the electron-to-baryon ratio $Y_e<0.5$. The matter ejected from the neutron star expands adiabatically and cools. If the temperature drops below $T\approx 0.5$ MeV, a network of nuclear reactions allows matter to flow to heavier nuclei which then become the seed for the *r* process. Obviously the *r* process requires $Y_e<0.5$, but, as has been recently pointed out by Meyer and collaborators, neutrino-induced reactions might also hinder the formation of an *r* process at this site [9]. To understand their argument, one has to consider that nucleosynthesis in this environment starts with assembling basically all free protons into ^{4}He. However, the charged current reactions on the remaining free nucleons (mainly neutrons) will then drive the value of Y_e closer to 0.5, possibly counteracting a successful *r* process [9].

There have been several suggestions for how neutrino-induced reactions can play a role during and even after the *r* process network. If the ejected matter flow reaches waiting-point nuclei associated with the magic neutron numbers $N=50$, 82, and 126 at rather small radii above the neutron star (say ≈ 100 km), ν_e-induced charged-current reactions can compete with the β decays of the longest lived waiting point nuclei and thus speed up the matter flow to heavier nuclei [10]. In the usual picture the *r* process stops when the neutron supply ceases (''freeze-out''). The produced very neutron-rich progenitor nuclei then undergo a series of β decays until they reach a stable nucleus whose calculated abundance can then be compared with observation. However, as discussed by Haxton and collaborators [11], if the *r* process occurs in an extreme neutrino flux, charged- and neutral-current neutrino reactions will alter the abundance distribution of the progenitor nuclei after freeze-out, as these neutrino-induced reactions can spallate neutrons out of the target nuclei. This ''post-processing'' is particularly important for the abundances of *r*-process nuclei with masses just below the abundance peaks at $A=130$ and 195. As neutron star mergers also produce strong neutrino fluxes, neutrino-

nucleus reactions will also be quite important during and after the *r*-process network in this scenario.

Recently Meyer, McLaughlin, and Fuller [9] have performed the first study of the *r* process within the neutrino-driven wind model in which they consistently considered ν_e-induced charged-current reactions. These authors computed the relevant neutrino-nucleus cross sections (including appropriate estimates of the number of neutrons emitted from the excited daughter nucleus) on the basis of the independent particle model [12]. Importantly this study indicates a less dramatic role played by neutrino-induced reactions than previously anticipated. Meyer *et al.* find that capture on free neutrons is at all stages of the *r* process within the neutrino-driven wind model more important than capture on nuclei. As a consequence, these authors point out that, if neutrino-induced reactions are invoked to accelerate the matter flow to heavier nuclei, the simultaneously occurring and stronger capture on neutrons drives the matter more proton-rich and thus counteracts a successful *r* process. A first attempt to include neutral-current spallation of neutrons from nuclei into the neutrino-driven wind model for the nuclear *r* process has been reported by Meyer *et al.* [13].

Meyer, McLaughlin, and Fuller [9], however, also point out that the sensitivity of the *r* process to neutrino irradiation means that neutrino-capture effects can strongly help to constrain the *r*-process site or neutrino physics. Here it is quite exciting to speculate that, in a scenario where electron neutrinos were converted to other neutrino species by matter-enhanced processes in the region above the neutron star surface [14], the large flux of antineutrinos would drive protons into neutrons ensuring a large initial neutron richness [9].

To explore these many interesting facets of neutrino-induced effects before, during and after the *r* process, and in the presence of neutrino oscillations or without, requires the availability of a rather reliable neutrino-nucleus reaction rate compilation. It is our aim here to improve the previous rate estimates by calculating the charged current (ν_e, e^-) and the neutral current (ν, ν') cross sections for the neutron-rich nuclei along the *r* process path, covering nuclei with neutron numbers $N=41-135$. The study of the (ν_e, e^-) reactions are strongly facilitated by two observations. At first, due to the rather low average energies ($\overline{E}=11$ MeV) the (ν_e, e^-) cross sections for supernova ν_e neutrinos are mainly given by allowed transitions. Secondly, the total strength of the two allowed transitions, Fermi and Gamow-Teller (GT), are governed by sum rules. For the Fermi transition, one has the usual $S_F=(N-Z)$ rule, where N,Z are the neutron and proton numbers of the parent nucleus. For the GT transition we note that, for extremely neutron-rich nuclei the GT_+ direction (in which a proton is changed into a neutron) is blocked. Hence the Ikeda sum rule reduces to an effective sum rule for the total GT_- strength, $S_{\mathrm{GT}_-}=3(N-Z)$. (For the same reasons, $\overline{\nu}_e$ induced charged-current reactions do not play a role in the *r* process.)

It has been noted previously [10,15] that a rough estimate of the allowed cross sections can be obtained if one employs these sum rules and the well-known energy parametrizations of the isobaric analog state (IAS) and the GT_- centroids [16]. While this procedure is a valid approximation for the Fermi contribution, which is totally concentrated in the IAS state, the GT_- strength is known to be fragmented over many states in the daughter nucleus, caused by the spin- and isospin-dependent parts in the residual interaction. In a first approximation, Qian *et al.* accounted for this fact by representing the GT_- distribution by a Gaussian with a width of a few MeV, centered around the parametrized centroid energy [10]. However, for very neutron-rich nuclei these centroid energies are at rather large excitation energies ($E_x \approx 20$ MeV), and thus weak contributions of the GT_- distribution leading to low-lying states in the daughter can be strongly amplified by phase space. Engel and Surman have investigated these contributions within the random phase approximation (RPA) and conclude that these low-lying transitions can increase the cross sections up to a factor of 2 [17]. They also find that nonallowed transitions do not contribute significantly to the total cross sections. Following Engel and Surman we will adopt the RPA approach to study charged current neutrino-nucleus reactions.

Neutral current reactions are mainly mediated by the ν_μ and ν_τ neutrinos and their antiparticles due to their significantly higher average energies. These energies are even sufficient to excite the giant dipole resonances in the nucleus. Hence the supernova neutral current reaction cross section is given basically by allowed Gamow-Teller and first-forbidden transitions. Studies of muon capture, which is also dominated by first-forbidden transitions, have shown that the RPA method is quite appropriate to describe these transitions at the involved momentum transfers. However, the RPA usually does not recover all correlations necessary to fully describe the quenching of the GT strength, which for neutral current is not governed by a sum rule. Clearly the method of choice to describe GT transitions is the interactive shell model [18] but such computationally intensive studies are prohibited for the large body of nuclei we are interested in. Thus we will use the RPA approach also to calculate neutral current cross sections.

Our paper is organized as follows. In the next section we will briefly recall the relevant formalism to calculate neutrino-nucleus cross sections and discuss details of our nuclear model. In Sec. III we present a selection of our extensive compilation covering the reaction cross sections for about 1000 nuclei.

II. THEORETICAL BACKGROUND

We are interested in three types of semileptonic processes: charged current neutrino scattering,

$$\nu + {}_Z X_N \rightarrow {}_{Z+1} X^*_{N-1} + e^-, \tag{1}$$

and inelastic neutral current neutrino and antineutrino scattering,

$$\nu + {}_Z X_N \rightarrow {}_Z X^*_N + \nu',$$

$$\overline{\nu} + {}_Z X_N \rightarrow {}_Z X^*_N + \overline{\nu'}. \tag{2}$$

In the derivation of the relevant cross sections we follow the description given by Walecka [19]. Hence we assume the standard current-current form for the Hamiltonian governing these reactions. After a multipole expansion of the weak nuclear current and applying the extreme relativistic limit (lepton energy $\epsilon_f \gg$ lepton mass $m_f c^2$) the neutrino (antineutrino) cross section for excitation of a discrete target state is given by [19,20]

$$\left(\frac{d\sigma_{i\to f}}{d\Omega_e}\right)_{\nu/\nu} = \frac{g^2\epsilon_f^2}{2\pi^2}\frac{4\pi\cos^2(\Theta/2)}{(2J_i+1)} \times F(Z,\epsilon_f)\left[\sum_{J=0}^{\infty}\sigma_{CL}^J + \sum_{J=1}^{\infty}\sigma_T^J\right]$$

$$\sigma_{CL}^J = \left|\langle J_f|\left|\tilde{M}_J + \frac{\omega}{|\vec{q}|}\tilde{L}_J(q)\right||J_i\rangle\right|^2,$$

$$\sigma_T^J = \left(-\frac{q_\mu^2}{2\vec{q}^2} + \tan^2\frac{\Theta}{2}\right) \times [|\langle J_f||\tilde{T}_J^{\mathrm{mag}}(q)||J_i\rangle|^2 + |\langle J_f||\tilde{T}_J^{el}(q)||J_J\rangle|^2] \mp \tan\frac{\Theta}{2}\sqrt{\frac{-q_\mu^2}{|\vec{q}|^2} + \tan^2\frac{\Theta}{2}} \times [2\,\mathrm{Re}\langle J_f||\tilde{T}_J^{\mathrm{mag}}(q)||J_i\rangle\langle J_f||\tilde{T}_J^{el}(q)||J_i\rangle^*]. \quad (3)$$

Here g is the universal coupling constant, Θ the angle between the incoming and outgoing lepton, and $q_\mu = (\omega, \vec{q})$ ($q := |\vec{q}|$) the four-momentum transfer. The minus sign refers to the neutrino cross section. The quantities $\tilde{M}_J$, $\tilde{L}_J$, $\tilde{T}_J^{el}$, and $\tilde{T}_J^{\mathrm{mag}}$ denote the multipole operators for the charge, longitudinal, and the transverse electric and magnetic parts of the four-current, respectively. Following Ref. [19] they can be written in terms of one body operators in the nuclear many-body Hilbert space. The cross section involves the reduced matrix elements of these operators between the initial state J_i and the final state J_f.

The Coulomb functions $F(Z,\epsilon)$ account for the Coulomb interaction between the final charged lepton and the residual nucleus in the charged-current processes. We treat them relativistically in the same manner as outlined in Ref. [21], i.e., we use the Coulomb correction derived by numerical solution of the Dirac equation for an extended nuclear charge [22]

$$F(Z,\epsilon) = F_0(Z,\epsilon)L_0$$

with

$$F_0(Z,\epsilon) = 4(2p_l R)^{2(\gamma-1)}\left|\frac{\Gamma(\gamma+iy)}{\Gamma(2\gamma+1)}\right|^2 e^{\pi\cdot y}, \quad (4)$$

where Z denotes the atomic number of the residual nucleus, ϵ the total lepton energy (in units of m_0c^2), and p_l the lepton momentum (in units of m_0c). R is the nuclear radius (in units of $\lambda = \hbar/m_0c$) and γ and y are given by (α=fine structure constant):

$$\gamma = \sqrt{1-(\alpha Z)^2}, \quad y = \alpha Z\frac{\epsilon}{p_l}. \quad (5)$$

The numerical factor L_0 in Eq. (4), which describes the finite charge distribution and screening corrections, is nearly constant (≈ 1.0), and can be well approximated by a weakly decreasing linear function in p_l. We calculate the differential cross section (3) as a function of the initial lepton energy ϵ_i, the excitation energy of the nucleus ω, and the scattering angle Θ. In the extreme relativistic limit ($\epsilon_f \gg m_f c^2$) the kinetic energy of the final lepton is then given by energy conservation as $\epsilon_f = \epsilon_i - \omega$ and the $|\vec{q}|$ value is

$$|\vec{q}| = \sqrt{\omega^2 + 4\epsilon_i\cdot(\epsilon_i-\omega)\sin^2\frac{\Theta}{2}}. \quad (6)$$

The total cross section is obtained from the differential cross sections by summing over all possible final nuclear states and by numerical integration over the solid angle $d\Omega$.

The distribution of the various supernova neutrino species is usually described by a Fermi-Dirac spectrum

$$n(\epsilon) = \frac{1}{F_2(\alpha)T^3}\frac{\epsilon^2}{\exp[(\epsilon/T)-\alpha]+1}, \quad (7)$$

where T, α are parameters fitted to numerical spectra, and $F_2(\alpha)$ normalizes the spectrum to unit flux. The transport calculations of Janka [23] yield spectra with $\alpha \sim 3$ for all neutrino species. While this choice also gives a good fit to the ν_e and $\bar{\nu}_e$ spectra calculated by Wilson and Mayle [24], their ν_x spectra favor $\alpha = 0$. In this work we will use both values for α.

The total cross section has then to be folded with the energy distribution of the incident neutrino beam $n(\epsilon)$ resulting in

$$\frac{d\bar{\sigma}}{d\omega}(\omega) = \int_\omega^\infty \frac{d\sigma}{d\omega}(\epsilon_i,\omega)n_i(\epsilon_i)d\epsilon_i. \quad (8)$$

As nuclear model we adopt the random phase approximation with proton/neutron formalism, i.e., we distinguish between proton and neutron degrees of freedom for the particle and hole states. In particular, in the charged current reaction our model changes a neutron particle in the parent nucleus to a proton hole state in the daughter. Our parent ground states are described by the lowest independent particle model state, assigning partial occupancy to the last shell if this is not completely occupied. The same shell is included among the hole states, but appropriately partially blocked [25]. The partial occupation formalism necessarily assumes that the parent ground state is spherical, what is often not the case for nuclei in the middle of major shells. As our total cross section results turn out to be rather smooth and not too sensitive on nuclear structure effects, we believe that the neglect of de-

formation in the parent ground states does not introduce too severe uncertainties. The particle and hole states have been determined from a Woods-Saxon potential with standard parameters. The depth of the potential has been adjusted to reproduce the proton and neutron separation energies in the parent nucleus. As residual interaction we used the Landau-Migdal force given in Ref. [26]. This parametrization has been chosen to reproduce simultaneously the energies of the IAS states in ^{48}Ca and ^{208}Pb. However, for the nuclei of interest here we had usually to slightly shift the hole energies to reproduce the position of the IAS state. For the nuclear binding energies we adopted the mass compilation of Duflo and Zuker [27].

In our calculations we considered all multipole transitions with $\lambda \leqslant 3$ and both parities. From shell model calculations it is well established that the Gamow-Teller strength requires an additional quenching factor which we take from Ref. [28] as $(0.7)^2$; this is often referred to as renormalization of the axialvector coupling constant. Hence the Ikeda sum rule is also modified by the same factor. For the other multipole operator, there exists no firm indication for a need of such an additional quenching factor. For example, muon capture rates, which are dominated by first-forbidden transitions, are well described by RPA calculations without quenching of the form factors [29]. For the q dependence of the nuclear form factors we use the standard dipole form.

We note that we use the appropriate multipole operators for finite momentum transfer [19]. Thus, only in the limit $q \rightarrow 0$ our 0^+ and 1^+ operators reduce to the Fermi and Gamow-Teller operators, respectively. Nevertheless for brevity we will in the following refer to the momentum-dependent 0^+ and 1^+ multipole operators as Fermi and Gamow-Teller operators. The effect of the finite-momentum transfer on these two transitions is discussed below.

As a consequence of the partial occupation formalism, our calculation always assigns the spin-parity 0^+ to the parent ground state. This is, of course, incorrect for odd-A and most odd-odd nuclei. Nevertheless this shortcoming is not expected to effect our results noticeably as data and shell model calculations, where available, indicate no differences in the gross structures of the multipole responses between even-even, odd-A, and odd-odd nuclei, although for the latter two cases the multipole strength is distributed over three different angular momenta in the daughter nucleus (e.g., Ref. [18], and references therein).

Most of the multipole transition strength for the neutrino-induced reactions studied here resides above particle (i.e., neutron) thresholds. Hence the excited daughter state will decay by emission of one or several neutrons. In the simplest approximation, the partial cross section for the emission of k neutrons is given by

$$\overline{\sigma}[\nu,e^-(kn)] = \int_{E_k}^{E_{k+1}} \frac{d\overline{\sigma}(\nu,e^-)}{d\omega} d\omega, \tag{9}$$

$$\overline{\sigma}[\nu,\nu'(kn)] = \int_{E_k}^{E_{k+1}} \frac{d\overline{\sigma}(\nu,\nu')}{d\omega} d\omega, \tag{10}$$

where the total charged current or neutral current cross section [$\overline{\sigma}(\nu,e^-)$ and $\overline{\sigma}(\nu,\nu')$, respectively] is integrated between the thresholds for the emission of k neutrons (E_k) and $k+1$ neutrons (E_{k+1}). Again we use the compilation of Duflo and Zuker to derive the relevant neutron thresholds in the neutron-rich nuclei. This mass compilation takes effects such as nuclear deformation and pairing into account.

III. RESULTS AND DISCUSSION

In this section we will give a sample of the results obtained in our intensive RPA calculations for the neutrino-induced charged and neutral current reactions on neutron-rich nuclei for the astrophysical r process. In total our study has been performed for about 1000 nuclei with neutron numbers between $N=41$ and 135. The cross sections have been calculated assuming a Fermi-Dirac distribution for the neutrinos with chemical potential $\alpha=0$ and $\alpha=3$, and for each of these values, temperatures $T=2.75$, 3.5, 4.0, 5.0, 6.4, 8.0, and 10.0 MeV. This grid includes the currently recommended neutrino spectra for supernova ν_e neutrinos ($T=4$ MeV, $\alpha=0$ [30] or $T=2.75$ MeV, $\alpha=3$ [23]), $\overline{\nu}_e$ neutrinos ($T=5$ MeV, $\alpha=0$ [30], $T=4$ MeV, $\alpha=3$ [23]), and ν_x neutrinos ($T=8$ MeV, $\alpha=0$ [30], and $T=6.4$ MeV, $\alpha=3$ [23]). Whereas all six neutrino types can contribute to neutral current reactions, only ν_e neutrinos, with the lowest average neutrino energy, can initiate charged-current reactions during the r process. For the other neutrinos charged current reactions are blocked either due to the extreme neutron excess of the parent nucleus or by the available energy which does not allow the production of a muon or τ lepton. However, in the exciting scenario that neutrino oscillations occur, it is conceivable that ν_x neutrinos change into ν_e neutrinos which then have significantly higher energies. Our (T,α) grid also allows us to explore the consequences of complete neutrino oscillations and we will show below that this leads to significant changes in the charged current cross sections.

A. Charged current reactions

In the following discussion we will at first assume a neutrino spectrum with $T=4$ MeV and $\alpha=0$. As expected, the charged current cross section for such supernova ν_e neutrinos is then dominated by allowed Fermi and GT transitions. This is demonstrated in Fig. 1 for the even isotopes with neutron number $N=82$. The energy scale refers to the excitation energy in the daughter nucleus. The energies of the hole states in the daughter have been chosen such that the IAS state is reproduced at the correct energy.

With increasing neutron excess or, equivalently, decreasing charge number the Q value increases more strongly then the slight decrease in the Coulomb energy associated with the IAS state. Consequently the IAS state moves to higher excitation energies in the daughter (from about 16 MeV in ^{132}Sn to 26 MeV in ^{122}Zr). The GT strength within the RPA is concentrated in two major transitions which are split by about 6 MeV. Strongly favored by phase space, a third GT transition at rather low excitation energies contributes to the

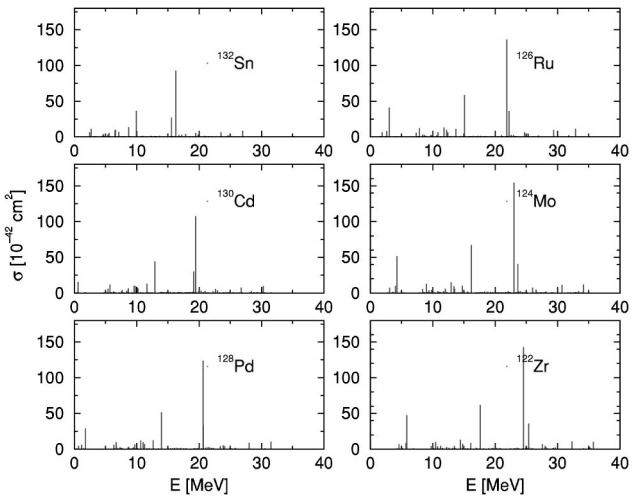

FIG. 1. Excitation functions for the (ν_e, e^-) reaction on even nuclei with neutron number $N=82$ calculated for supernova ν_e neutrinos with a Fermi-Dirac spectrum characterized by the parameters $T=4$ MeV and $\alpha=0$. The scale refers to excitation energies in the daughter nucleus.

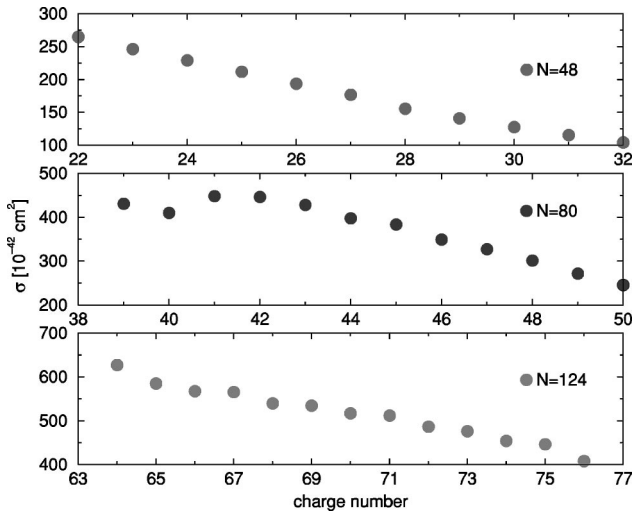

FIG. 2. Total (ν_e, e^-) cross sections for neutron-rich nuclei with neutron numbers $N=48$, 80, and 124. The calculation has been performed for supernova ν_e neutrinos characterized by a Fermi-Dirac spectrum with $T=4$ MeV and $\alpha=0$.

cross sections. In these nuclei, this transition involves the change of a $g_{7/2}$ neutron into a $g_{9/2}$ proton and hence this cross section contribution increases from ^{132}Sn (where it is absent) to ^{122}Zr, associated with the decreasing filling of the $g_{9/2}$ orbital in the parent nucleus. We remark that with increasing charge number the Fermi transition requires an increasingly larger neutrino energy. As a consequence the Fermi transition to the IAS state does not contribute significantly to the charged current cross section for nuclei in the $N=126$ region where the correspondingly larger Z values ($Z\approx 70$ for *r*-process nuclei) places the IAS at an energy about 15 MeV above the parent ground state, which is hardly reachable for supernova ν_e neutrinos with an average energy of 11 MeV.

Although from experimental (p,n) studies the relation between the GT centroid and the IAS energy is well established (e.g., Ref. [31])

$$E_{\mathrm{GT}} - E_{\mathrm{IAS}} = 7.0 - 28.9\frac{N-Z}{A}\ [\mathrm{MeV}], \qquad (11)$$

it has been controversially discussed whether $E_{\mathrm{GT}} - E_{\mathrm{IAS}} < 0$ in very neutron-rich nuclei (e.g., Ref. [10]) or $E_{\mathrm{GT}} - E_{\mathrm{IAS}} = 0$ (e.g., Ref. [9]). Our RPA calculations confirm the assumption made by Qian *et al.* [10], i.e., $E_{\mathrm{GT}} - E_{\mathrm{IAS}} < 0$ in nuclei with extreme neutron excess. We note that the same result is found in large-scale shell model calculations in lighter, very neutron-rich nuclei such as ^{60}Mn [32].

As stated above, our formalism considers the finite-momentum transfer dependence of the operators. To study the importance of this treatment we have performed a calculation of the nucleus ^{132}Sn in which we have replaced the 0^+ and 1^+ multipole operators by the genuine Fermi and GT operators. In this $q=0$ limit, the cross sections for these operators reduce to formula (4) in Ref. [10]. For both operators we find a reduced cross section if the finite momentum-transfer is considered and, of course, this reduction increases with momentum transfer. For example, our cross sections are about 20% smaller for supernova ν_e neutrinos with $T=4$ MeV than those calculated for pure Fermi or GT operators, while the reduction amounts to roughly 100% for $T=8$ MeV ν_e neutrinos. The reduction is mainly caused by the destructive interference with higher-order operators such as $\tau\vec{r}\cdot\vec{p}$ and $\tau\vec{\sigma}\vec{r}\cdot\vec{p}$.

In Fig. 2 we discuss the dependence of the ν_e-induced cross sections on the charge number. As examples we have chosen isotone chains with $N=48$, 80, and 124, close to the magic neutron numbers related to the three pronounced *r*-process abundance peaks. Strikingly the cross sections increase approximately linear with decreasing charge number. This has two reasons. At first, the total transition strength for both dominating multipoles (Fermi, GT) are bound by sum rules which are proportional to $(N-Z)$. Secondly, the position of the GT centroids and the IAS energies, relative to the parent ground state, are lowered in energy, roughly proportional to *Z*. As the neutron excess increases with the larger mass number for the nuclei shown in Fig. 2, the total cross sections are largest for the nuclei with $N=124$. Shell effects influence the total cross sections only slightly; an example is ^{120}Zr in Fig. 2.

We would like to remark that the obviously smooth dependence on the charge number within an isotone chain, reflecting basically the smooth dependence of the cross section on the sum rules and on the positions of IAS and GT centroid, suggests that our incorrect treatment of the ground state spins for odd-*A* and odd-odd nuclei does not introduce noticeable inaccuracies in the cross sections. We mention that our charged-current cross sections are somewhat larger than the estimates obtained in Ref. [9] on the basis of the independent particle model. However, the agreement for those nuclei which we have compared [33] has always been better than 50%. Thus we do not expect that the conclusions drawn in [9] will change if our neutrino-nucleus rate compi-

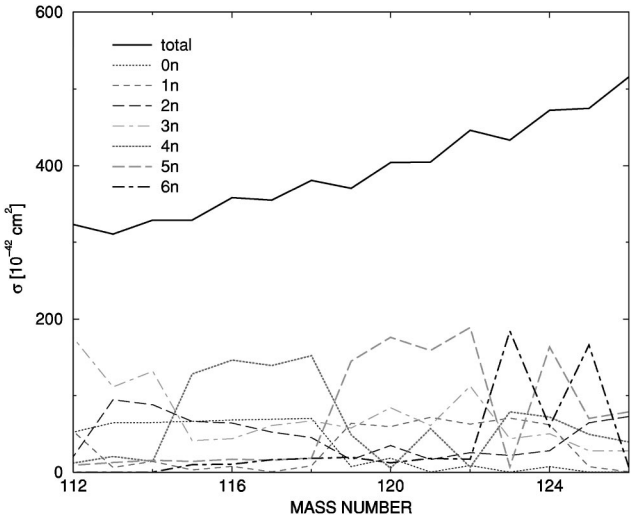

FIG. 3. Total (ν_e,e^-) and partial neutron-emission cross sections for neutron-rich molybdium isotopes. The calculations have been performed for supernova ν_e neutrinos characterized by a Fermi-Dirac spectrum with $T=4$ MeV and $\alpha=0$.

lation will be used rather than the independent particle model estimates.

Figure 3 uses the molybdium isotopes as an example to discuss the dependence of the partial cross sections $\overline{\sigma}[\nu_e,e^-(kn)]$ on the neutron excess. Again, the total cross sections increase with the neutron number for the reasons discussed above. However, for the partial cross sections it is relevant that the excitation energies of the IAS and the GT centroids, relative to the daughter ground state, increase with increasing neutron excess, due to larger mass differences (Q values). At the same time, the daughter nuclei move closer to the neutron dripline. Hence, the neutron threshold energies are reduced and as a consequence the average number of neutrons spallated by the (ν_e,e^-) reaction increases with neutron excess. While, for example, the largest partial cross section in ^{113,114}Mo is found in the $[\nu_e,e^-(2n)]$ channel, this maximum is shifted to the $5n$ channel for $^{118-122}$Mo and to the $6n$ channel for the Mo isotopes with the largest neutron excess. Note that the neutron threshold energies have a rather strong odd-even staggering introduced by pairing effects. Therefore the Fermi and the strong GT transitions, although at energies above the threshold for emission of k neutrons in a certain nucleus, can be below this threshold in the neighboring nucleus with one neutron more. This behavior explains the staggering in the results for the emission of 5 and 6 neutrons, respectively, observed in the $^{123-125}$Mo isotopes.

In passing, we note that the nucleus ^{124}Mo corresponds to the magic neutron number $N=82$. As can be observed in Fig. 3, the neutron shell closures are not emphasized in (ν_e,e^-) cross sections which behave smoothly across the magic neutron numbers. This is different from β decay where half-lives are relatively longer at the neutron shell closures. Hence the pronounced peaks in the r-process abundance distributions, related to the magic neutron numbers, show that at freeze-out β-decay dominates over charged-current neutrino reactions in the r process.

TABLE I. Average number of spallated neutrons $\langle k\rangle$ for (ν_e,e^-) reactions on neutron-rich nuclei with neutron numbers $N=50$ (left), $N=82$ (middle), and $N=126$ (right). The calculations have been performed for supernova ν_e neutrinos characterized by a Fermi-Dirac spectrum with $T=4$ MeV and $\alpha=0$.

Z	$\langle k\rangle$	Z	$\langle k\rangle$	Z	$\langle k\rangle$
34	0.68	50	1.57	76	2.31
33	1.45	49	2.40	75	2.66
32	0.98	48	2.30	74	2.55
31	1.72	47	2.49	73	3.12
30	1.69	46	2.42	72	3.01
29	2.62	45	3.29	71	3.89
28	2.54	44	3.12	70	3.80
27	3.64	43	4.07	69	4.57
26	3.50	42	4.13	68	4.54
25	5.02	41	5.44	67	5.26
24	4.89	40	5.40	66	5.20
23	6.80			65	6.21
22	6.84				

The same trend as derived from Fig. 3 can be observed in Table I which shows the average number of spallated neutrons in the (ν_e,e^-) reaction

$$\langle k\rangle=\frac{\sum_k k\times\overline{\sigma}[\nu_e,e^-(kn)]}{\sum_k \overline{\sigma}[\nu,e^-(kn)]} \tag{12}$$

for selected nuclei with neutron numbers $N=50$, 82, and 126. Thus, charged-current neutrino reactions on r-process nuclei can spallate about 2–6 neutrons out of the parent nucleus. The pairing effect introduces an odd-even dependence in the neutron thresholds, which is clearly reflected in the $\langle k\rangle$ values.

Our choice of nuclei allows us to compare the results with those published in Ref. [10]. The study of these authors differs from ours in two aspects. At first, Ref. [10] only considered the genuine Fermi and GT contributions to the charged-current cross sections, neglecting the finite momentum-transfer effects as discussed above. Further, the GT response has been described by a Gaussian distribution of 5 MeV width, centred around the empirical GT centroid energy [e.g., Eq. (11)]. As has already been pointed out in Ref. [17], the neglect of low-lying GT transitions underestimates the cross sections by up to a factor of 2. This effect for the total cross sections is, however, partially cancelled, as Ref. [10] adopted a smaller universal quenching factor of $(1.25)^{-1}$ for the GT operator which appears too small compared to recent shell model results [28]. On the other hand, Qian *et al.* treated the particle decays of the excited states in the daughter nucleus more consistently than we do here, as these authors employ a statistical model to follow the sequential decays. Satisfyingly, we find that despite our crude approximation in treating the particle decay, our results for

TABLE II. Various multipole contributions to the total (ν_e, e^-) cross sections for ^{74}Fe (left), ^{124}Mo (middle), and ^{192}Er. The calculations have been performed for ν_e neutrinos with a Fermi-Dirac spectra with $\alpha=0$ and $T=4$ MeV and $T=8$ MeV, respectively.

Multipole	$T=4$ MeV	$T=8$ MeV	$T=4$ MeV	$T=8$ MeV	$T=4$ MeV	$T=8$ MeV
0^+	30.9	163.4	39.4	294.8	28.0	334.5
0^-	0.0	0.6	0.3	2.3	5.5	15.6
1^+	127.8	460.3	309.5	1124	358.5	1708
1^-	11.4	236.7	32.5	591	52.2	929
2^+	1.7	7.5	5.8	200.5	10.2	378
2^-	20.1	259.9	53.5	687.5	76.7	1109
3^+	1.3	60.0	4.4	173	7.0	295
3^-	0.1	17.3	0.5	54.5	13.0	110
Total	193.4	1206	445.9	3128	551.1	4880

the average number of spallated neutrons $\langle k \rangle$ agrees reasonably well with the values found by Qian *et al.* Closer inspection finds that our values are usually slightly larger than those of Ref. [10] caused by the contributions of first-forbidden transitions.

In the exciting scenario, in which $\nu_x \leftrightarrow \nu_e$ oscillations occur, supernova ν_e neutrinos can have the high-energy ν_x neutrino distribution when passing through the region above the neutron star in which the *r* process possibly occurs. The average neutrino energy of the ν_e neutrinos in this case is then 25 MeV, which has significant consequences for the charged-current reaction rates. This is exemplified in Table II which compares the multipole break-down of the total (ν_e, e^-) cross section for selected nuclei calculated for ν_e neutrinos with $T=4$ MeV and $T=8$ MeV (in both cases we adopted $\alpha=0$).

At first, Table II confirms again that the cross section for the $T=4$ MeV ν_e neutrinos is dominated by Fermi and GT transitions which contribute roughly 75% to the total cross sections. (Note that the ratio of Fermi to GT contributions decrease with increasing charge number for the reasons explained above.) The remaining contributions stem mainly from the 1^- and 2^- multipoles, including low-lying dipole strengths. The centroid of the dipole strength can be approximated as [34]

$$E_{\rm dip} = 31.2A^{-1/3} + 20.6A^{-1/6} \ \text{MeV} \qquad (13)$$

and is higher than the centroid of the GT strength. Hence it can hardly be reached by the available neutrino energies for the $T=4$ MeV spectrum. This situation changes drastically if in a potential neutrino oscillation scenario the average ν_e neutrino energy increases to 25 MeV. Then transitions to the giant dipole resonances contribute significantly to the total cross sections, as can be seen in Tables II and III. Furthermore, the total charged-current cross section increases by about an order of magnitude. The number of spallated neutrons $\langle k \rangle$, however, grows less dramatically, from $\langle k \rangle = 2-6$ to $\langle k \rangle = 3-7$, as the sequential neutron decays lead to daughter nuclei with increasingly larger neutron thresholds.

B. Neutral current

The neutral-current reactions can be induced by all three neutrino flavors and their antiparticles, but due to phase space considerations they are dominated in a supernova by the neutrino species with the largest average energy (ν_x neutrinos in the case without oscillations). The results which we present in this subsection have been calculated for a neutrino or antineutrino spectrum with $T=8$ MeV and $\alpha=0$. The relatively large neutrino energies allow then for the excitation of the giant dipole resonances and indeed these transitions, together with the GT multipole, dominate the cross sections. This is exemplified in Fig. 4 for the neutral $(\overline{\nu}, \overline{\nu'})$ cross sections for selected even nuclei with neutron number $N=82$. The GT multipole induces two strong transitions at excitation energies around $E_x=6-7$ MeV and at 9 MeV. The lower of these transitions involve the $g_{9/2} \rightarrow g_{7/2}$ excitation of a proton, while the other is initiated by the $h_{11/2} \rightarrow h_{9/2}$ excitation of a neutron. As in our model the $g_{9/2}$ proton orbital is being filled when moving from ^{122}Zr to ^{132}Sn, this proton excitation is absent in ^{122}Zr and its strength and excitation energy increases with increasing filling of the $g_{9/2}$ orbital (in ^{124}Mo this transition corresponds to a peak in the cross section at 5.5 MeV with 2.7×10^{-42} cm^2, while in

TABLE III. Average number of spallated neutrons $\langle k \rangle$ for (ν_x, ν_x') reactions on neutron-rich nuclei with neutron numbers $N=50$ (left), $N=82$ (middle), and $N=126$ (right). The calculations have been performed for supernova ν_x neutrinos characterized by a Fermi-Dirac spectrum with $T=8$ MeV and $\alpha=0$.

Z	$\langle k \rangle$	Z	$\langle k \rangle$	Z	$\langle k \rangle$
34	1.09	50	1.48	76	1.52
33	1.30	49	1.57	75	1.69
32	1.32	48	1.76	74	1.77
31	1.39	47	1.93	73	1.85
30	1.44	46	2.01	72	2.05
29	1.72	45	2.28	71	2.26
28	1.86	44	2.49	70	2.53
27	2.06	43	2.67	69	2.60
26	2.43	42	2.88	68	2.74
25	2.68	41	3.11	67	2.86
24	2.94	40	3.51	66	3.05
23	3.25			65	3.24
22	3.71				

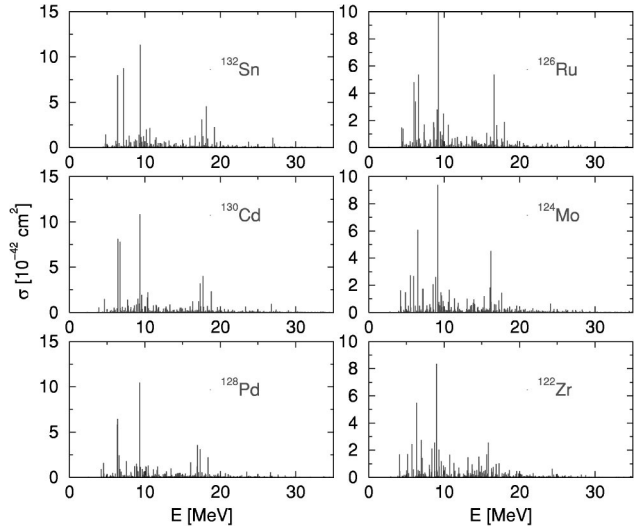

FIG. 4. Excitation functions for the $(\overline{\nu},\overline{\nu'})$ reaction on even nuclei with neutron number $N=82$ calculated for supernova neutrinos with a Fermi-Dirac spectrum characterized by $T=8$ MeV and $\alpha=0$.

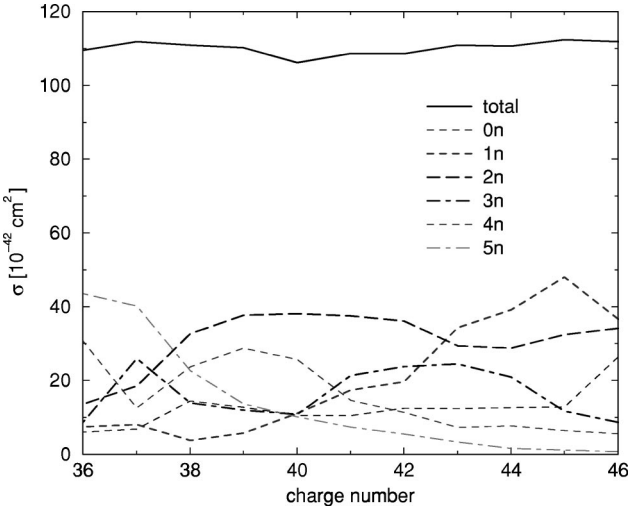

FIG. 6. Total (ν,ν') and partial neutron-emission cross sections for neutron-rich isotones with neutron number $N=72$. The calculations have been performed for supernova ν_x neutrinos characterized by a Fermi-Dirac spectrum with $T=8$ MeV and $\alpha=0$.

^{130}Cd it is at 6.7 MeV with 7.7×10^{-42} cm^2). The dipole (1^-) transitions have a strong contribution due to the giant dipole resonance which in these nuclei is fragmented over a few states in the energy range $E_x\approx16-18$ MeV. Due to the E_ν^2 dependence of the phase space, low-lying 1^- strength, mainly in the energy range $E_x=5-8$ MeV, also contributes noticeably to the cross section, as does low-lying 2^- multipole strength.

Figure 5 compares the total neutral current cross sections for the same three isotone chains (with $N=48$, 80, and 124) as displayed in Fig. 2. The cross sections increase with growing charge number, or more precisely, with increasing mass number. In fact, we find that the total (ν,ν') cross section is roughly proportional to the mass number, where our calculation estimates the proportionality factor to be about 0.9 for neutrinos with a Fermi-Dirac distribution and the parameters $T=8$ MeV, $\alpha=0$. Haxton and collaborators [30,10,35] have explained this behavior by recognizing that the (ν_x,ν_x') cross section is dominated by first-forbidden transitions, which, when approximately described within the Goldhaber-Teller model, obeys the Thomas-Reiche-Kuhn sum rule. This sum rule is proportional to [30,35] $NZ/A=(A/4)(1-[(N-Z)/A]^2$. Thus even for very neutron-rich nuclei with $N\approx2Z$, the proportionality $NZ/A\sim A/4$ is good within about 10%. As the GT contribution to the cross section involves only the valence nucleons, a universal scaling of this partial cross section with A cannot be expected. However, the variations in the GT part are small enough not to disturb the approximate scaling of the total (ν_x,ν_x') cross section with A. However, the GT transitions dominate the total cross sections for neutrino spectra with small average energies, for example for supernova ν_e neutrinos. In this case the neutral current does not scale with A anymore and becomes rather sensitive to the nuclear structure involved.

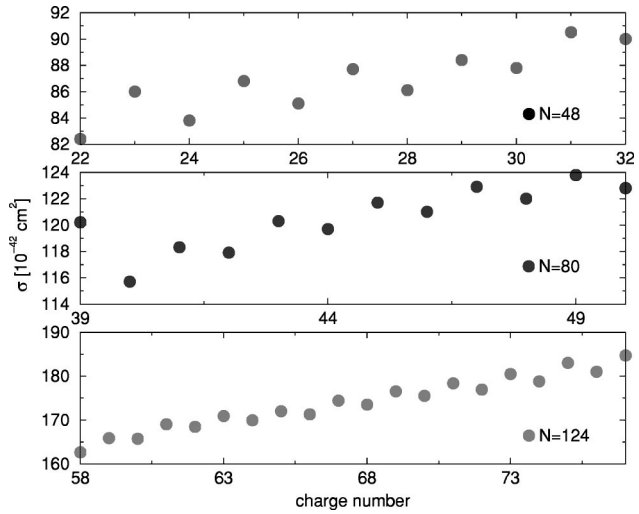

FIG. 5. Total (ν,ν') cross sections for neutron-rich nuclei with neutron numbers $N=48$, 80, and 124. The calculation has been performed for supernova neutrinos characterized by a Fermi-Dirac spectrum with $T=8$ MeV and $\alpha=0$.

Figure 5 also shows a slight odd-even staggering of the (ν_x,ν_x') cross sections: the cross section for an odd parent nucleus is about 1% larger than the average of the two neighboring even nuclei. This effect reflects the pairing dependence in the nucleon separation energies to which we have adjusted our potential depth.

Figure 6 displays the total cross section $\overline{\sigma}(\nu,\nu')$ and the partial cross sections for the emission of k neutrons, $\overline{\sigma}[\nu,\nu'(kn)]$, for the isotone chain with neutron number $N=72$. While the total cross sections show only small variations, the neutron emission cross sections exhibit the expected behavior. With increasing neutron excess (decreasing charge number) emission of a larger number of neutrons increases on the expense of the few-neutron channels. Differently than for the charged-current (e.g., Fig. 3), the centroid

energies of the multipole excitations vary only mildly within the isotone chain. Thus the increase in the average number of emitted neutrons is dominantly due to the fact that the neutron separation energies are getting smaller with increasing neutron excess as one moves closer to the neutron dripline. Furthermore $\langle k \rangle$ is noticeably smaller for (ν_x, ν_x') reactions on very neutron-rich nuclei than for the charged-current reaction (compare to Table I). The reason is simply due to the fact that, for the charged-current reactions, the excitation energies in the daughter nucleus are additionally pushed up by the significant Q values.

For inelastic neutrino scattering on nuclei, the vector and axial-vector amplitudes to the cross section interfere constructively, while they interfere destructively for inelastic scattering with antineutrinos. Therefore inelastic antineutrino cross sections on nuclei are smaller than the corresponding neutrino cross sections. However, this effect is rather small (usually less than 30%) as the (ν_x, ν_x') cross section is dominated by axial-vector contributions.

IV. CONCLUSION

In both currently discussed scenarios, the neutrino-driven wind model above a new born neutron star in a type II supernova and neutron star mergers, the nuclear *r* process is expected to occur in the presence of extreme neutrino fluxes. Consistent and dynamical studies of the *r* process in either of the two scenarios thus need the input of the relevant neutrino-nucleus rates for the involved neutron-rich nuclei. To determine these rates we have calculated the total cross sections and the partial cross sections for the emission of k neutrons for (ν_e, e^-) and (ν, ν') reactions on about 1000 neutron-rich nuclei with neutron numbers $N=41$–135. The cross sections have been determined assuming a Fermi-Dirac spectrum for the neutrinos with parameters for temperature and chemical potential which include those currently favored for supernova neutrinos. The charged-current (ν_e, e^-) cross sections have also been calculated for the high-energy $\nu_{\mu,\tau}$ spectra to allow the exploration of neutrino-induced effects in the presence of (complete) neutrino oscillations.

To realize such a computationally intense program, the choice for the nuclear model is dictated by the balance between reliability and computational feasibility. We have chosen the random phase approximation which has been used rather successfully before in the study of neutrino-nucleus reactions (we note that the continuum version of the RPA agrees rather well in its cross section predictions with the conventional RPA model used here) and which fulfills the relevant sum rules for the involved multipole strengths. Our calculations included allowed (Fermi and Gamow-Teller) and forbidden transitions. While the (ν_e, e^-) cross sections are dominated by allowed transitions, first-forbidden transitions dominate the (ν_x, ν_x') cross sections (and the charged-current cross sections if complete $\nu_x \rightarrow \nu_e$ oscillations occur). A compilation of our cross section tables will be published elsewhere. An electronic file with the cross section data can be obtained from the authors upon request.

We find that both types of supernova neutrino-nucleus reactions are quite effective in spallating neutrons out of *r*-process nuclei. While a (ν_x, ν_x') reaction knocks out about three neutrons from nuclei along the *r*-process path at freeze-out (these are nuclei with neutron separation energies about 2–3 MeV [4]), the (ν_e, e^-) reaction is more efficient as the rather large Q value in these nuclei places the giant resonance excitations quite high in the daughter nucleus (in excess of 20 MeV). As a consequence, the charged-current reaction knocks out 5–6 neutrons. While these reactions can alter the *r*-process distribution of progenitor nuclei by post-processing, e.g., Refs. [10,11], the neutrino-induced neutron spallation is not sufficient to shift material from the $A=130$ peak region to fill up the so-called *r*-process abundance trough around $A=115$. This is more likely related to nuclear structure effects, as for example shell quenching effects as discussed in Ref. [36].

While our study covers the nuclei involved in the *r*-process network, neutrino-induced reactions on other nuclei play also a role during a type-II supernova. Charged-current (ν_e, e^-) reactions on lighter nuclei ($A<60$) can occur during the α-process network, which proceeds the *r* process in the neutrino-driven wind model and generates the seed nuclei, and within the neutrino nucleosynthesis [30]. These scenarios involve nuclei closer to stability. As Gamow-Teller transitions will significantly contribute to the relevant cross sections and since the GT_+ transitions are no longer blocked for nuclei close to stability, the calculation of these neutrino-nucleus cross sections requires an improved nuclear model. We have recently proposed that an approach in which GT transitions are described within the interactive shell model and forbidden transitions within the random phase approximation reproduces neutrino-nucleus cross sections quite well [37]. We are currently in the process to calculate neutrino-nucleus reaction cross sections for nuclei with $A<60$ within such a hybrid model. Finally neutrino reactions on heavier nuclei ($A>60$) within a type-II supernova might be responsible for the synthesis of certain nuclides such as ^{138}La and ^{180}Ta [30]. It is therefore desirable to extend the present calculation also towards the stable region of the nuclear chart. The RPA approach appears still appropriate for this endeavour. However, for nuclei closer to stability the decay of the excited states will involve the competition of several particle channels and a treatment of these decays within a proper statistical model approach is indispensable.

ACKNOWLEDGMENTS

The authors would like to thank Petr Vogel for useful discussions and Gail McLaughlin for providing us with some of the neutrino-nucleus cross sections obtained within the independent particle model. This work has been partly supported by a grant of the Danish Research Council and by the Swiss National Science Foundation. A.H. thanks the Danish Rector's Conference for financial support and the Institute of Physics and Astronomy at the University of Aarhus for its hospitality.

[1] E. M. Burbidge, G. R. Burbidge, W. A. Fowler, and F. Hoyle, Rev. Mod. Phys. **29**, 547 (1957).
[2] A. G. W. Cameron, Chalk River Report No. CRL-41, 1957 (unpublished).
[3] F.-K. Thielemann, M. Arnould, and J. W. Truran, in *Advances in Nuclear Astrophysics*, edited by E. Vangioni-Flam *et al.* (Editions Frontieres, Gif sur Yvette, 1987), p. 525.
[4] J. J. Cowan, F.-K. Thielemann, and J. W. Truran, Phys. Rep. **208**, 267 (1991).
[5] S. E. Woosley, G. J. Mathews, J. R. Wilson, R. D. Hofmann, and B. S. Meyer, Astrophys. J. **433**, 229 (1994).
[6] K. Takahashi, J. Witti, and H.-Th. Janka, Astron. Astrophys. **286**, 857 (1994).
[7] R. Rosswog, M. Liebendörfer, F.-K. Thielemann, M. R. Davies, W. Benz, and T. Piran, Astron. Astrophys. (to be published), astro-ph/9811367.
[8] Y.-Z. Qian, Nucl. Phys. **A621**, 363c (1997); Y.-Z. Qian and S. E. Woosley, Astrophys. J. **471**, 331 (1996).
[9] B. S. Meyer, G. McLaughlin, and G. M. Fuller, Phys. Rev. C **58**, 3696 (1998).
[10] Y.-Z. Qian, W. C. Haxton, K. Langanke, and P. Vogel, Phys. Rev. C **55**, 1532 (1997).
[11] W. C. Haxton, K. Langanke, Y.-Z. Qian, and P. Vogel, Phys. Rev. Lett. **78**, 2694 (1997).
[12] G. M. Fuller and B. S. Meyer, Astrophys. J. **453**, 792 (1995).
[13] B. S. Meyer, G. J. Mathews, W. M. Howard, S. E. Woosley, and R. D. Hoffman, Astrophys. J. **399**, 656 (1992).
[14] G. C. McLaughlin, J. Fetter, B. Balantekin, and G. M. Fuller, Phys. Rev. C **59**, 2873 (1999).
[15] G. C. McLaughlin and G. M. Fuller, Astrophys. J. **455**, 202 (1995); G. M. Fuller and B. S. Meyer, *ibid.* **453**, 792 (1995).
[16] G. F. Bertsch and H. Esbensen, Rep. Prog. Phys. **50**, 607 (1987).
[17] R. Surman and J. Engel, Phys. Rev. C **58**, 2526 (1998).
[18] E. Caurier, K. Langanke, G. Martinez-Pinedo, and F. Nowacki, Nucl. Phys. **A653**, 439 (1999).
[19] J. D. Walecka, *Semi-Leptonic Weak Interactions in Nuclei in Muon Physics*, edited by V. W. Hughes and C. S. Wu (Academic, New York, 1975).
[20] J. S. Connell, T. W. Donnelly, and J. D. Walecka, Phys. Rev. C **6**, 719 (1972).
[21] W. C. Haxton, G. J. Stephenson, Jr., and D. Strottman, Phys. Rev. D **25**, 2360 (1982).
[22] H. Behrens and W. Bühring, *Electron Radial Wave Functions and Nuclear Beta-Decay* (Clarendon, Oxford, 1982).
[23] H.-T. Janka and W. Hillebrandt, Astron. Astrophys. **224**, 49 (1989); H.-T. Janka and W. Hillebrandt, Astron. Astrophys., Suppl. Ser. **78**, 375 (1989).
[24] J. R. Wilson (private communication), as cited in Ref. [10].
[25] D. Rowe, Rev. Mod. Phys. **40**, 153 (1968).
[26] G. A. Rinker and J. Speth, Nucl. Phys. **A306**, 360 (1978); M. R. Plumlet *et al.*, Phys. Rev. C **56**, 263 (1997).
[27] J. Duflo and A. P. Zuker, Phys. Rev. C **59**, R2347 (1999); **52**, R23 (1995).
[28] G. Martinez-Pinedo, A. Poves, E. Caurier, and A. P. Zuker, Phys. Rev. C **53**, R2602 (1996).
[29] E. Kolbe, K. Langanke, and P. Vogel, Phys. Rev. C **50**, 2576 (1994); (unpublished).
[30] S. E. Woosley, D. H. Hartmann, R. D. Hoffman, and W. C. Haxton, Astrophys. J. **356**, 272 (1980).
[31] K. Nakayama, A. Pio Galeao, and F. Krmpotic, Phys. Lett. **114B**, 217 (1982).
[32] K. Langanke and G. Martinez-Pinedo, Nucl. Phys. A (to be published).
[33] G. C. McLaughlin (private communication).
[34] T. W. Donnelly, J. Dubach, and W. C. Haxton, Nucl. Phys. **A251**, 353 (1975).
[35] G. M. Fuller, W. C. Haxton, and G. C. McLaughlin, Phys. Rev. D **59**, 085005 (1999).
[36] B. Chen, J. Dobaczewski, K.-L. Kratz, K. Langanke, B. Pfeiffer, F.-K. Thielemann, and P. Vogel, Phys. Lett. B **355**, 37 (1995).
[37] E. Kolbe, K. Langanke, and G. Martinez-Pinedo, Phys. Rev. C **60**, 052801 (1999).